Open Peer Review on Qeios

Integration and Implementation of Multiple Soil Sensors for Automated and Regulated Irrigation

Sunday Samuel Adeosun[1], Samouel Olugbenga Oladele[1], Theophilus Ewetumo[1], Olurotimi Akintunde Dahunsi[1]

1 Federal University of Technology, Akure

Funding: No specific funding was received for this work.

Potential competing interests: No potential competing interests to declare.

Abstract

Agriculture is a critical sector contributing significantly to the global economy and food security. However, it faces several challenges such as climate change, water scarcity, soil nutrient depletion, and others. Efficient water management and nutrient monitoring are essential for sustainable agricultural practices; therefore, the main purpose of this research is to develop and evaluate an affordable wireless communication system for controlling irrigation and monitoring soil properties, including moisture, and essential nutrients such as nitrogen, phosphorus, and potassium (NPK). The performance of the prototype equipment was evaluated through field testing and validation. The developed system showcased a coefficient of determination for the selected soil parameters ranging from a very strong (0.98) R^2 to a strong R^2 (0.88) when compared with the standard measurement. It was observed that the developed system addressed the limitations of conventional soil monitoring methods, which often lack real-time and in-situ measurement capabilities. By automating the monitoring process, the system enabled precise irrigation scheduling, optimized water usage, and reduced wastes. Additionally, the real-time nutrient data facilitate site-specific fertilizer application, promoting sustainable and efficient agricultural practices. The developed system also enables users to make informed decisions regarding irrigation scheduling, fertilizer application, and crop management, ultimately leading to increased crop yields, reduced input costs, and minimized environmental impacts. The system's affordability and wireless communication capabilities will make it accessible to a broader range of agricultural stakeholders, fostering sustainable and efficient farming practices.

Adeosun, Sunday Samuel[1,*], **Oladele, Samouel Olugbenga**[2], **Ewetumo, Theophilus**[3], and **Dahunsi, Olurotimi Akintunde**[4]

[1]*Mechanical Engineering Department, Federal University of Technology, Akure.*

[2]*Agricultural Engineering Department, Federal University of Technology, Akure.*

[3]*Physics Electronics Department, Federal University of Technology, Akure.*

[4]*Mechatronics Engineering Department, Federal University of Technology, Akure.*

[*]samakay8@gmail.com

1. Introduction

Agriculture plays a vital role in the global economy and food security but is challenged by climate change, water scarcity, and soil nutrient depletion. Sustainable practices require effective water management and nutrient monitoring. This research aims to create and assess an affordable wireless communication system for irrigation control and soil property monitoring, focusing on moisture and key nutrients like nitrogen, phosphorus, and potassium (NPK).

Overwhelming floods, extreme hurricanes, warm winds, reduced rainfall, and other climatic shifts severely impact crop performance and disrupt plant life cycles. Freshwater scarcity threatens food security and sustainable development, especially with the projected global population reaching 9.8 billion by 2050 (United Nations, 2017). Efficient water use and conservation for irrigation are crucial to boost food production and prevent water scarcity crises (Tsang & Jim, 2016). Rainfall and irrigation remain key water sources for agriculture.

There are three main methods of irrigation, which include surface, sprinkler, and drip irrigation, as shown in Figure 1.

Figure 1. a) Surface irrigation b) Sprinkler irrigation c) Drip irrigation

Surface irrigation is the most water-intensive irrigation method, with minimal water reaching plant roots and most flowing past through furrows. This temporary soil saturation hinders water absorption, making intermittent watering more efficient. Sprinkler irrigation loses significant water to evaporation as much of it falls on and evaporates from leaves. In contrast, drip irrigation is the most advanced system, delivering water directly to the crop's root zone, although excess water can cause nutrient leaching. Therefore, a controlled irrigation system is crucial for crop cultivation, supplementing natural rainfall. Irrigation is essential for supplying the precise water needed for plant growth (Oborkhale et al., 2015; Shibusawa, 2001). To enhance productivity and overcome farming challenges, the Internet of Things (IoT) is increasingly applied in agriculture. IoT provides farmers with extensive data and insights on soil properties, helping manage irrigation and soil nutrient depletion effectively. The physical and chemical properties measurement is of great importance for applications in the field of agriculture, allowing farmers to more efficiently manage irrigation systems and soil nutrients. Several studies have explored the use of sensor networks, microcontrollers, and IoT technologies for monitoring soil moisture and automating irrigation systems (Aziz et al., 2009; Dursun et al., 2011; Kumbhar & Ghatule, 2013; Shabadi & Patil, 2014; Payero et al., 2017; Krishnan et al., 2020; Naeem et al., 2021). These systems typically employ soil moisture sensors to measure the moisture content and trigger irrigation when the soil becomes too dry. Duarte and Coaguila Nuñez (2024)

focused specifically on the calibration of low-cost soil moisture sensors, which is an important aspect of ensuring accurate measurements. Research on the use of sensors for measuring soil NPK (nitrogen, phosphorus, and potassium) levels has explored various techniques and approaches. Some studies have focused on ion-selective electrodes, optical sensors, and spectroscopic methods for nitrogen measurement (Muñoz-Huerta et al., 2013; Padilla et al., 2018). Others have developed integrated systems that combine electrochemical sensors with mobile navigation for soil NPK data acquisition and mapping (Dai et al., 2020).

While these studies have made significant contributions to the development of sensors and techniques for measuring soil NPK levels, temperature, and moisture in separate research efforts, there is a need for a more comprehensive system that can not only measure and monitor soil NPK but also integrate other critical soil parameters such as soil moisture, pH, temperature, and electrical conductivity, with the capability to control irrigation equipment based on real-time soil data and transmit soil property data to users' mobile phones for quick and easy accessibility in any part of the country. The specific objectives are to: (a) identify the measurands, develop, source, and adapt appropriate sensors for monitoring some selected soil properties, (b) develop an integrated soil property data acquisition and wireless transmission system for (a) above, (c) develop a real-time data analysis and situation monitoring computer-based user platform, and (d) evaluate the performance of the prototype equipment.

2. Methodology

2.1. System Architecture

The system structure is made up of a basic circuit created to manage the irrigation system on a farm. It is designed to measure selected soil parameters, monitor, and control irrigation based on a response to the real-time status of soil moisture. The system uses radio communication to transmit information on soil moisture, temperature, nitrogen, phosphorus, pH, and electrical conductivity, as well as water level data, to local storage, a mobile phone, and a computer for further data analysis. The system performs the action of irrigation management by setting the threshold value of soil moisture. Accordingly, when the sensed moisture value goes below the threshold value, the controller checks the temperature, the user is alerted, and irrigation will commence only if the sensed soil moisture value is lower than the defined threshold value.

Figure 2 depicts the basic blocks of a low-cost automated irrigation and soil nutrient measurement system. The temperature sensor (DS18B20), 7-in-1 soil nutrients sensor (comprising soil moisture, soil temperature, electrical conductivity of the soil, soil pH, nitrogen, phosphorous, and potassium), soil moisture sensors for three levels, relay control circuit, surface moisture setting with rotary switch, Arduino Mega 2560 microcontroller, graphical liquid crystal display (GLCD), SIM800 module for remote monitoring, real-time clock, and power supply.

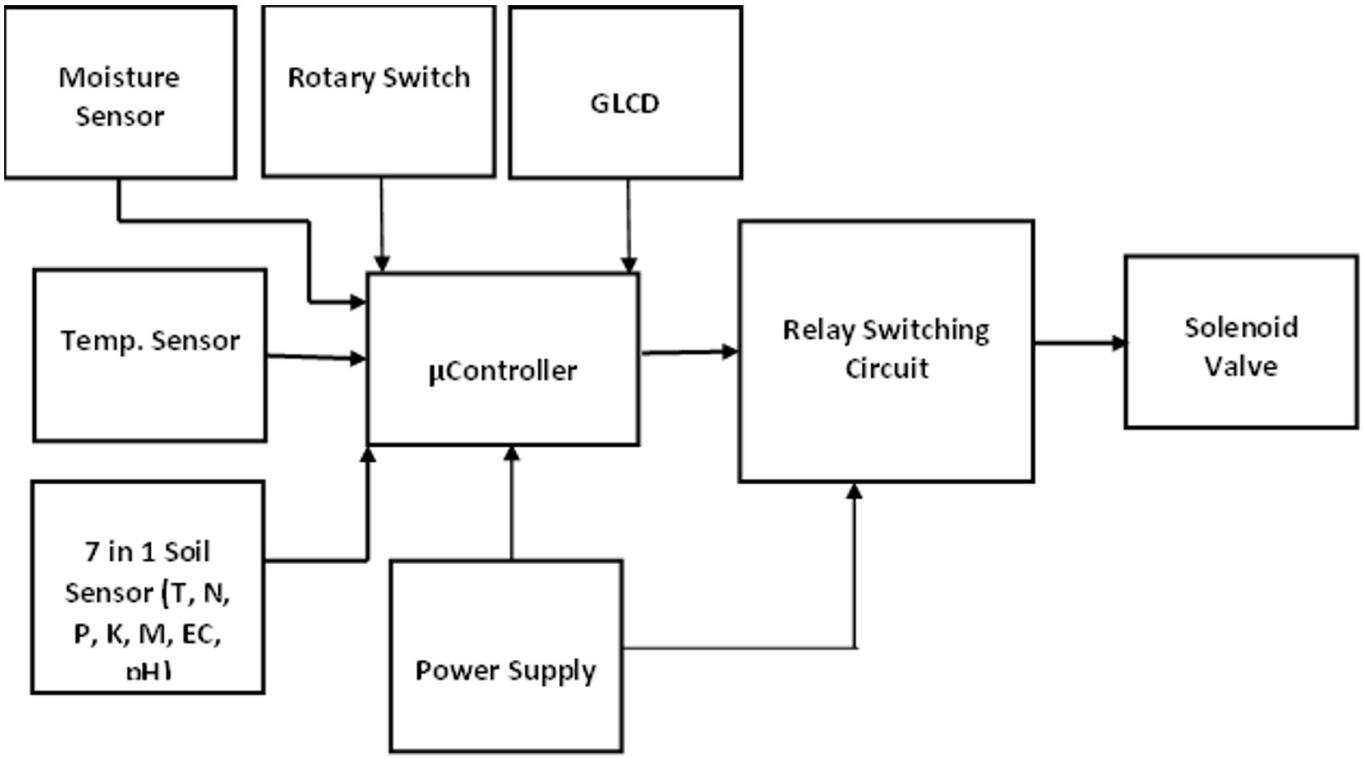

Figure 2. Block diagram of an automated irrigation and soil nutrient measurement system.

The structure of the system includes a basic circuit intended for managing irrigation on farmland. The IoT sensing unit comprises multiple sensors that collect data from the real world. This is followed by an embedded system that controls the physical aspects of the IoT application, the communication network, the protocol needed to transmit data to the internet, and data analysis.

2.1.1. Hardware development and integration

The system hardware, as shown in Figures 3 and 4, consists of different sensors such as soil moisture sensors, temperature sensors, and a 7-in-1 soil sensor which includes nitrogen, phosphorus, potassium, soil electrical conductivity, moisture, and pH, an Arduino board, and other components using the Internet of Things (IoT). The IoT manages all background tasks. Various sensors connected to the IoT device gather field data and relay it to the IoT system. This setup uses an Arduino Mega and GSM module to connect to the network. Data from temperature sensors, soil moisture sensors, and a seven-in-one soil sensor is transmitted to and stored in a database, and then shared with users through the network established by the SIM 800 module.

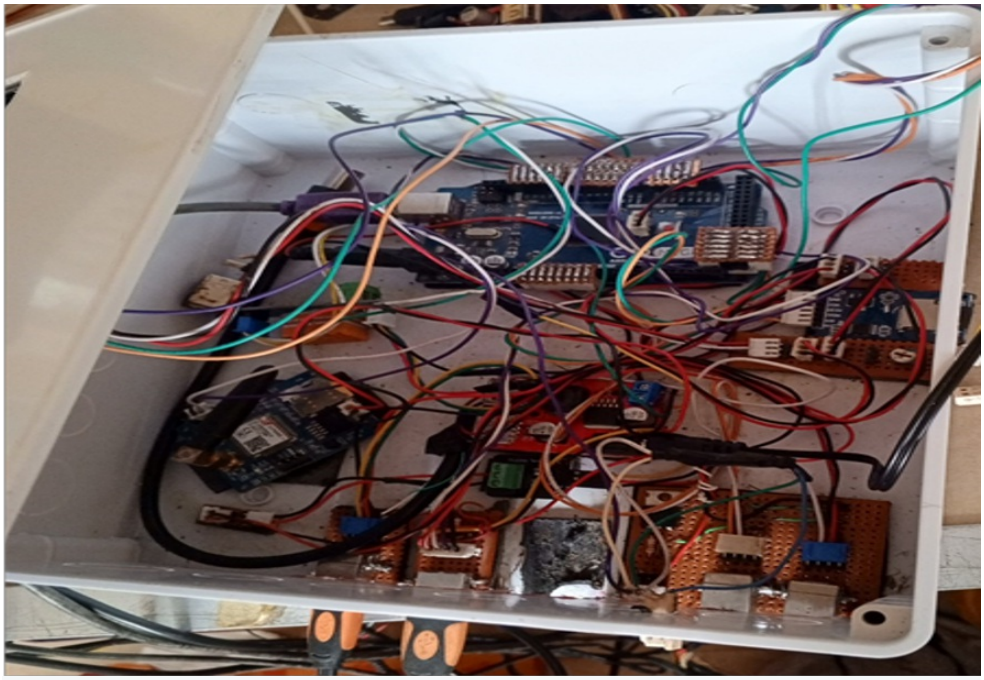

Figure 3. System circuit connections

Figure 4. Soil sensors

2.1.1.1. Hardware components

Soil temperature sensor

The DS18B20 is a direct-to-digital temperature sensor, as shown in Figure 5. It offers user-configurable resolution of 9, 10, 11, or 12 bits, corresponding to increments of 0.5°C, 0.25°C, 0.125°C, and 0.0625°C, respectively, with a default

resolution of 12 bits at power-up. Upon powering up, the DS18B20 enters a low-power idle state. To start a temperature measurement and A-to-D conversion, the master issues a Convert T [44h] command. The resulting data is stored in the 2-byte temperature register in the scratchpad memory, and the sensor returns to idle. If externally powered, the master can issue "read time slots" after the Convert T command; the DS18B20 transmits 0 during conversion and 1 when complete. This technique is not available with parasite power, as the bus must be held high during the entire conversion process.

Figure 5. Diagram of DS1820B temperature sensor

Relay switch and its circuit

Figure 6 illustrates a typical relay switch circuit. The relay connects to a 12V power source and the collector of transistor Q. The microcontroller’s digital pin links to the base of Q via a 1 kΩ resistor, acting as a switch. When the digital pin is high, the base-emitter junction of Q is forward-biased, turning Q on and allowing current to flow through the relay from the power supply to the emitter. When the digital pin is low, the base-emitter junction is reverse-biased, turning Q off, stopping the current, and switching off the relay. The relay's state is controlled by the microcontroller’s digital pin. Diode D is placed across the relay to protect the transistor from damage caused by the relay's back EMF when it turns off suddenly.

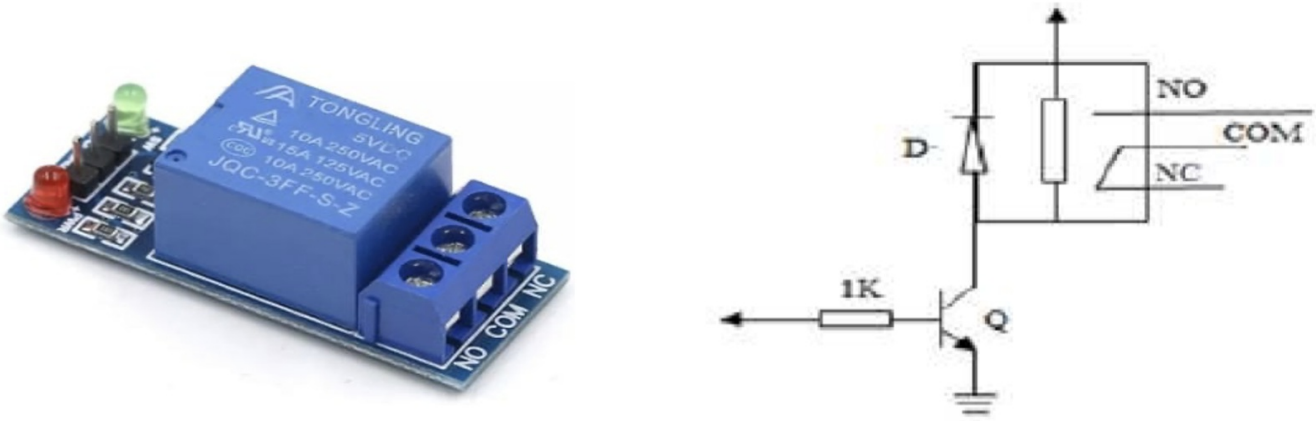

Figure 6. Relay Switch and its circuit

Rotary switch encoder for setting moisture

The rotation of the disk generates pulses in both the data transmission (DT) and clock (CLK) pins, with one pin's pulse delayed by 90 degrees relative to the other, depending on the rotation direction. By comparing these pulses, the direction of the encoder's rotation can be determined, though the exact position of the knob cannot be pinpointed—only the direction from the previous position. The disk can rotate either clockwise or counterclockwise. If DT transitions from high to low and CLK matches DT, the rotation is clockwise; if DT remains unchanged while rotating counterclockwise, DT goes from high to low while CLK stays high. These pulse patterns facilitate the development of an algorithm to identify rotational direction. The rotary encoder includes a switch for selecting maximum and minimum moisture values by pressing and releasing it while turning the spindle. Figure 7 depicts a typical rotary switch encoder.

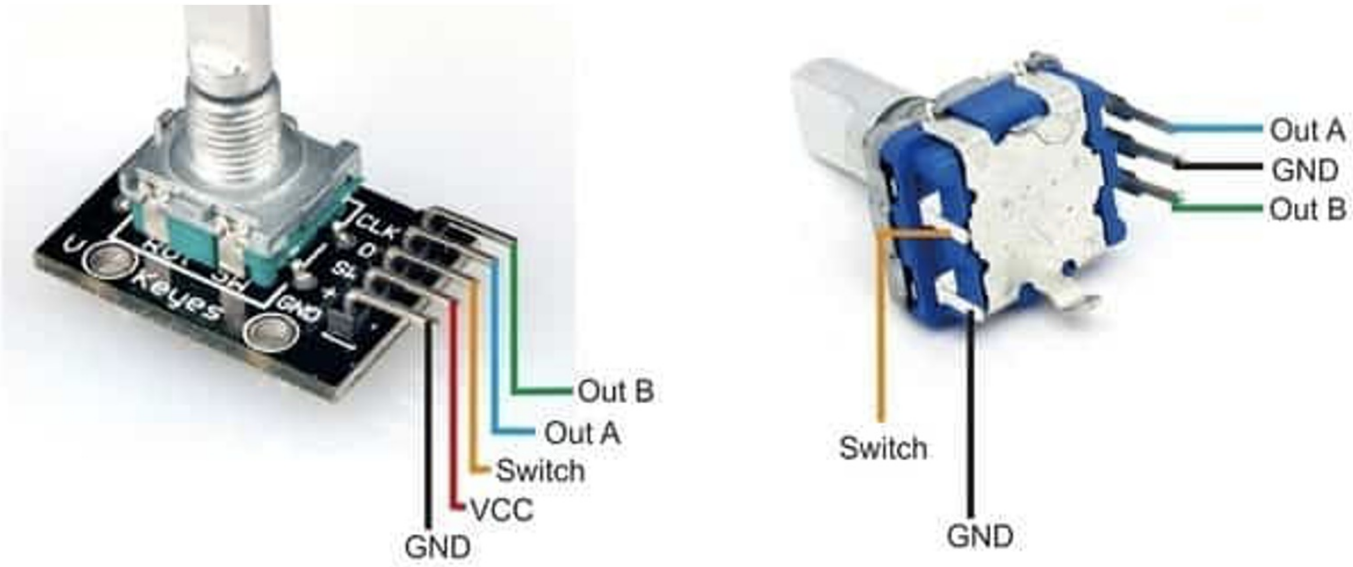

Figure 7. Rotary switch encoder

RS485 to TTL converter

Serial Interface RS485, as shown in Figure 8, is used for serial communications over longer distances between the microcontroller and the RS-485 output sensor. The converter is conveniently used for scientific sensor, office, and industrial applications (non-isolated) and provides superior characteristics/features normally found only on more expensive units.

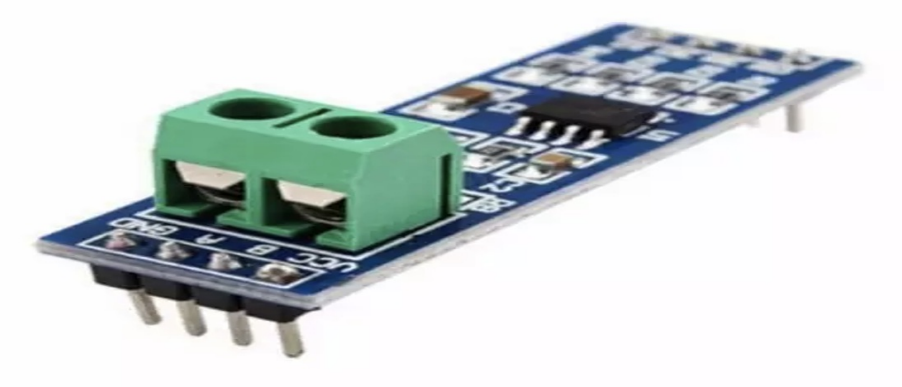

Figure 8. RS485 to TTL converter

Specifications and features of RS-485 are:

i. Compatibility: Converts RS485 to TTL and vice versa (transceiver function).
ii. RS485 Interface: 2-pin (A+B-) terminal connector.
iii. TTL Interface: 4-pin header (5V, GND, Tx, Rx).
iv. Transmission Rate: 300 - 115200 bps.
v. Transmission Distance: RS485 up to 1200m.
vi. Working Mode: Asynchronous, half-duplex, differential transmission.
vii. Operating Voltage: 5V DC.

7-in-1 Soil Monitoring Sensor

The 7-in-1 soil sensor, shown in Figure 9, monitors soil NPK, pH, electrical conductivity, temperature, and moisture content with high accuracy, fast response, and stable output. It is designed for long-term burial in soil, resistant to electrolysis and corrosion, vacuum-potted, and completely waterproof. Applications include scientific experiments, water-saving irrigation, greenhouse management, rapid soil measurement in pastures, plant cultivation, grain storage, and measuring moisture content and temperature of various particles. The sensor outputs via RS-485, necessitating an RS-485 to TTL bidirectional converter for interfacing with a microcontroller.

Figure 9. 7-in-1 Soil Monitoring Sensor

The 7-in-1 soil monitoring sensor has the following merits over the electrolytic type of soil sensor.

i. High precision agriculture sensors, rapid response, good exchangeability.
ii. Good tightness, corrosion resistance, the soil tester can be used in the soil for a long time.
iii. Flame retardant epoxy resin curing, completely waterproof, the soil tester can withstand strong external impact; and
iv. Steel needles are made of high-quality materials that can withstand long-term electrolysis, acid and alkali corrosion in soil.

Capacitive Soil Moisture Sensor

The soil volumetric water content (VWC) will be measured at four different depths (x, r, y, and z cm) using sensors. The moisture sensors measure VWC by measuring the dielectric constant of the media using capacitance/frequency domain technology. They need 2.5 - 3.6 VDC (10 mA) as input, and their output voltage is proportional to the VWC and the input voltage. When the output voltage from the sensor is lower than the preset threshold, the microcontroller automatically triggers the solenoid valve and stops the flow automatically when the soil moisture reaches the required level. The sensors were designed to work in the temperature range of –40˚C to +50˚C, requiring a measurement time of 10 milliseconds. Several commercial data loggers are capable of sampling and recording data from the moisture sensors. Figure 10 shows the conceptual measurement structure for the moisture and temperature sensors.

Figure 10. Capacitive soil moisture sensors

Solenoid Valve

Figure 11 is a 12V DC 1/2-inch solenoid water valve switch (Normally closed) that controls the flow of water and acts as a valve between pressure fluid.

Figure 11. Solenoid valve

LCD Display Serial Graphic Display 128x64 ST7920, White on Blue

The ERM12864SBS-6, shown in Figure 12, features a blue background with 128x64 monochrome white pixels and an ST7920 controller. It includes 8192 16x16 dot Chinese fonts and 126 16x8 dot half-height alphanumeric fonts. The display supports 6800 4-bit/8-bit parallel and 3-wire serial SPI interfaces. It has a single white LED backlight that can be easily dimmed with a resistor or PWM. The STN-blue LCD is negative, operates over a wide temperature range, and is ROHS

compliant. It offers optional 3.3V or 5V power supply configurations.

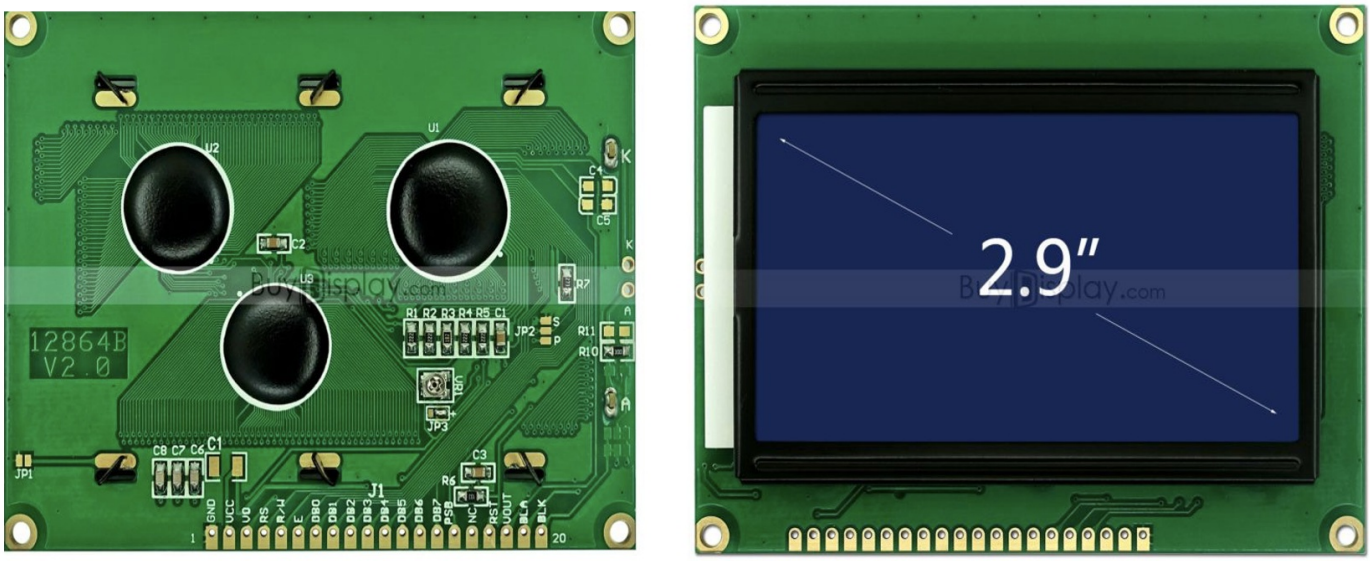

Figure 12. LCD Display

DS3231 RTC Module

Figure 13 displays the DS3231 serial real-time clock (RTC), a low-power device featuring a full binary-coded decimal (BCD) clock/calendar with 56 bytes of non-volatile (NV) static RAM (SRAM). It communicates via a bidirectional I²C bus for address and data transfer. The clock/calendar provides precise information on seconds, minutes, hours, day, date, month, and year. It automatically adjusts month-end dates for months with fewer than 31 days, including leap year corrections. The DS3231 supports both 24-hour and 12-hour time formats with AM/PM indication. It includes a built-in power-sense circuit that detects power failures and seamlessly switches to a backup supply, ensuring uninterrupted timekeeping operation.

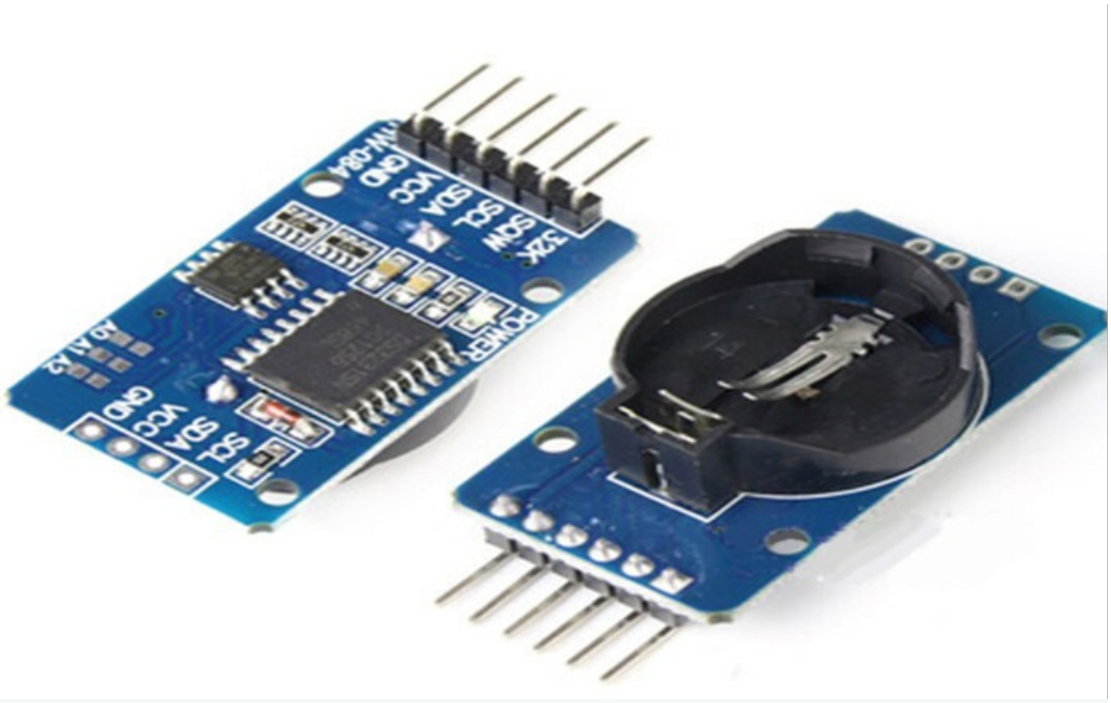

Figure 13. DS3231 RTC Module

GSM wireless module (Sim 800C)

The SIM800C is a quad-band GSM/GPRS module in a castellated hole package. It has stable performance, small size, and cost-effectiveness, and can meet diverse needs. The SIM800C operates at GSM/GPRS 850/900/1800/1900MHz and can be used worldwide for voice, SMS, and data transmission, with low power consumption which makes it suitable for a variety of compact product designs.

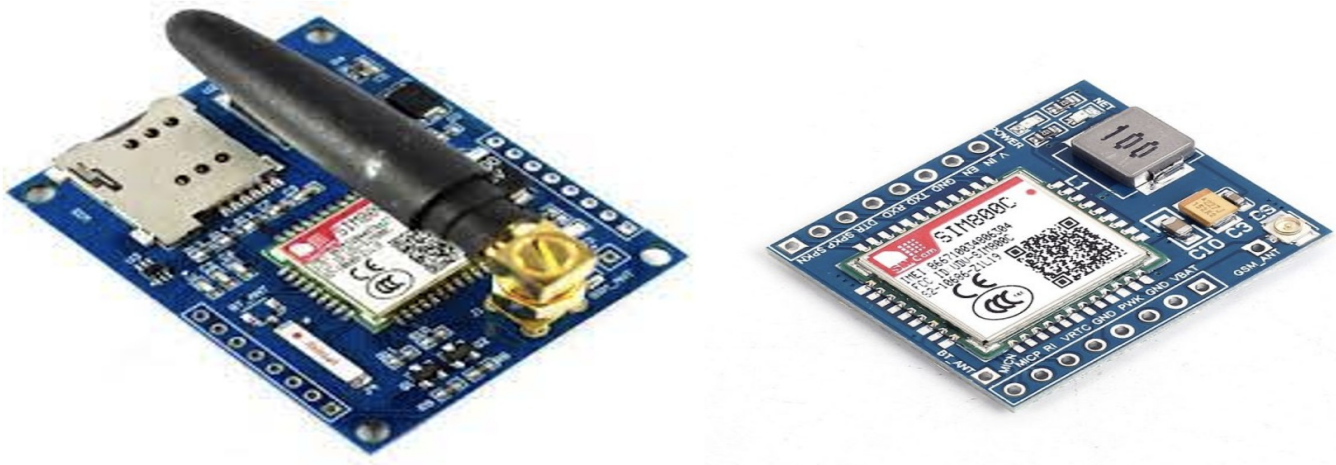

Figure 14. GSM wireless module (Sim 800)

SD card shield

The SD card shield provides storage space for the microcontroller, which allows users to read/write to an SD card via

Arduino's built-in SD library. It supports SD, SDHC, and Micro SD cards. It will only occupy the SPI port of the Arduino. A typical SD card shield is shown in Figure 15.

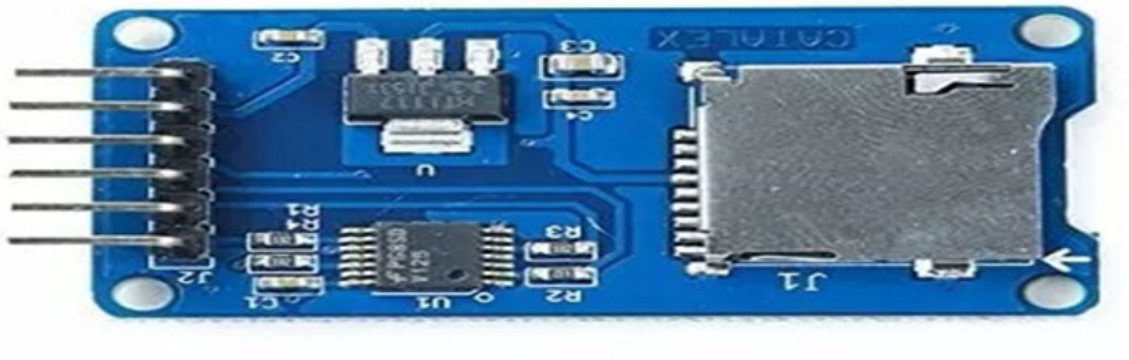

Figure 15. SD card shield

Arduino Mega

Figure 16 illustrates a microcontroller, a critical component in controlling specific functions within a device. It interprets data from its input/output (I/O) peripherals using its central processor. Temporary data received by the microcontroller is stored in its data memory, accessible to the processor for processing using instructions stored in its program memory. Subsequently, it utilizes its I/O peripherals to communicate and execute the necessary actions based on the interpreted data. This process enables the microcontroller to effectively manage and control various tasks within the device it operates in.

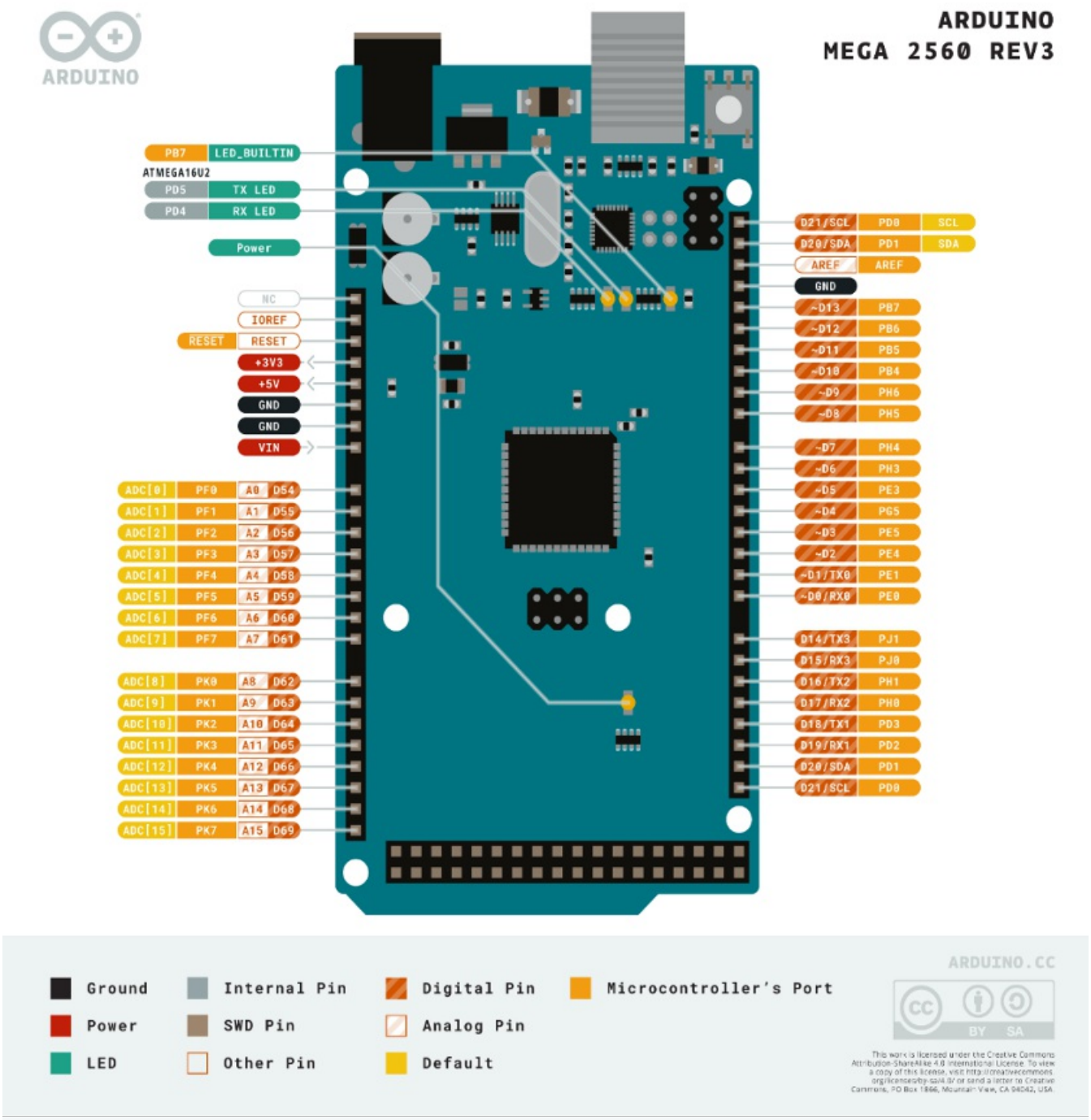

Figure 16. Arduino Mega

ATmega8 Microcontroller

The ATmega8, shown in Figure 17, is a low-power CMOS 8-bit microcontroller based on the AVR RISC architecture. By executing powerful instructions in a single clock cycle, the ATmega8 achieves throughputs approaching 1 MIPS per MHz, allowing the system designer to optimize power consumption versus processing speed.

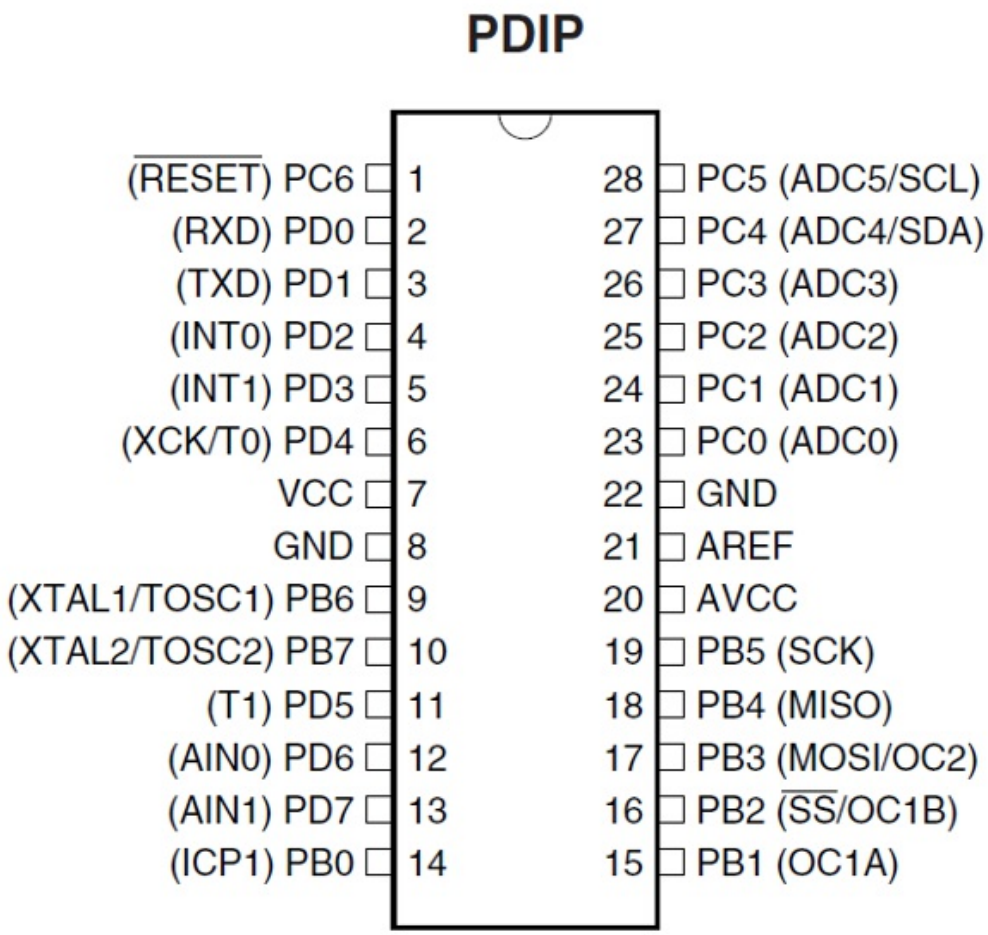

Figure 17. Pin diagram of ATmega8 microcontroller

JST XH 2.54mm Pitch Plug and Socket with Cable

The 2, 3, 4 shown in Figure 18, pin JST XH 2.54mm pitch plug and socket with cable, is often used in electronics projects to connect components such as sensors, solenoid valves, motors, LED strips, and other devices. The standardized pitch and secure locking mechanism make it convenient for both prototyping and permanent installations.

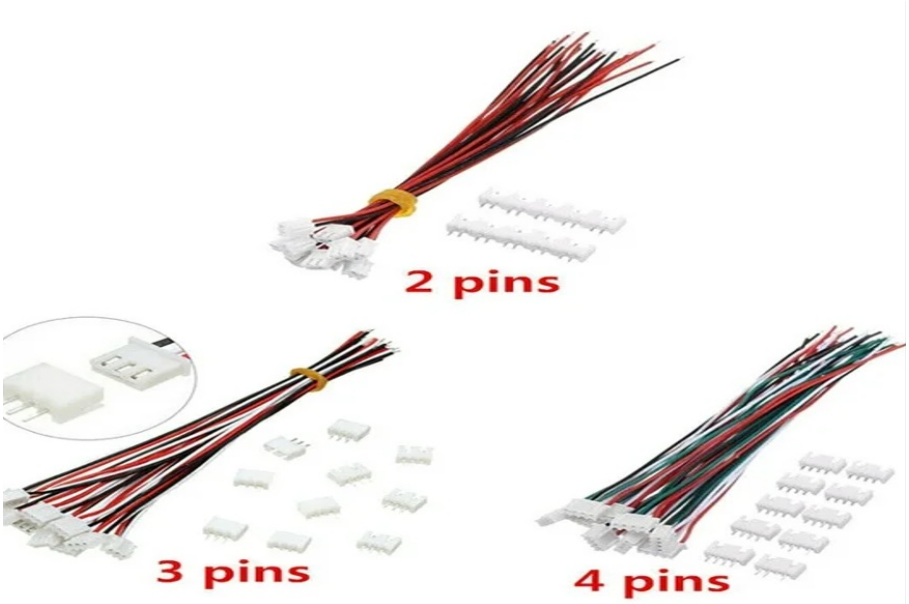

Figure 18. JST XH 2.54mm pitch plug and socket with cable

12V 4A AC Power Supply Adapter

The device depicted in Figure 19, also known as an AC adapter, power adapter, or charger, is used to convert alternating current (AC) from a wall outlet into direct current (DC) for electronic devices like computers, laptops, and smartphones. Adapters for battery-powered devices are often referred to as chargers or rechargers. Electronic devices that do not have internal components for voltage regulation rely on AC adapters for power. The internal circuitry of an external power supply is similar to that of a built-in power supply. External power supplies can be used with equipment that has an alternative power source, as well as with battery-powered devices to charge the battery while powering the equipment when plugged in.

Figure 19. 12V 4A power supply adapter

Button Switch

Push buttons, shown in Figure 20, are normally open tactile switches. Push buttons are those switches that enable us to activate the circuit or establish a specific connection only when they are pressed. Normally, the circuit appears connected when the button is pressed and disconnected when it is released. When wiring between the power supply and the circuit, it is important to ensure that the wires are connected to both terminals of the push-button switch.

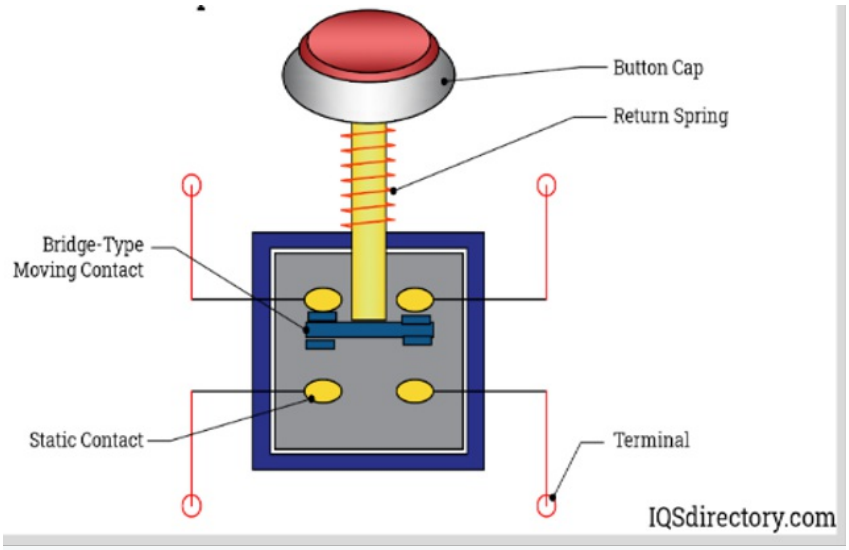

Figure 20. Button

2.1.2. Software Component

The software component is a modular, self-contained unit of software that encapsulates a specific set of related functionalities or services. These components work together to enable the device to perform its core functions, such as interfacing with sensors, acquiring and processing sensor data, storing and managing data, communicating with external systems, providing user interfaces, analyzing and reporting soil data, wirelessly sending soil data to a mobile phone, and managing the overall system operations.

2.2. Sensor Network Design and Deployment

The sensor network design of the soil monitoring system is shown in Figure 21.

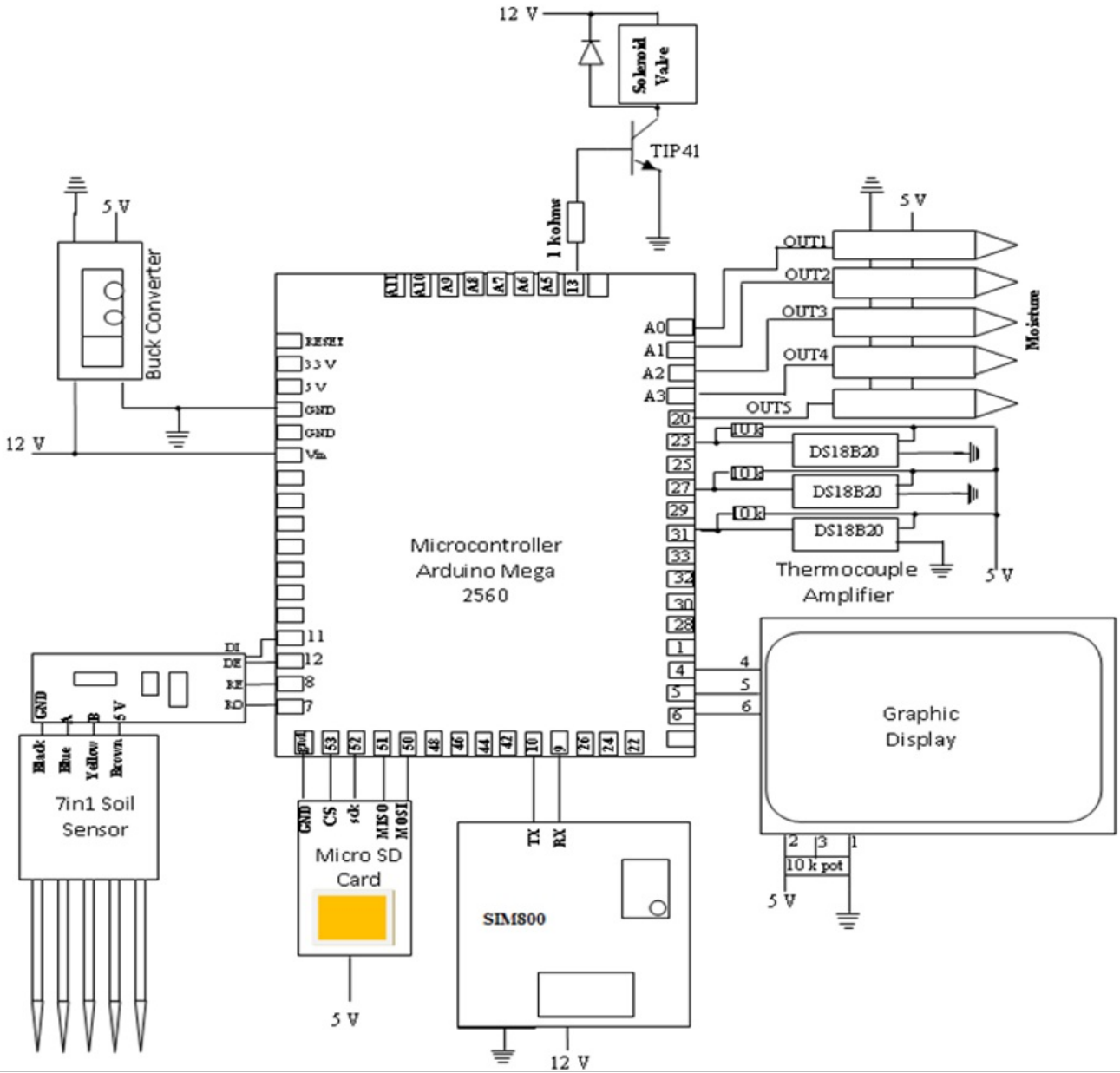

Figure 21. Sensor network design

Figures 22 – 23 show the set-up of the irrigation system and the developed system deployment to the field for testing. The experimental irrigation set-up typically includes an irrigation system to deliver water, designated experimental plots or field, equipment for water control, soil moisture and nutrients monitoring sensors, and a control system.

Figure 22. Set-up of the irrigation system

Figure 23. Soil sensor buried into the ground

2.3. Data Acquisition and Processing

The data collection and transmission system comprises sensors for moisture, NPK, pH, and electrical conductivity, alongside a microcontroller, local storage, and a SIM module. The microcontroller operates the sensors at 3.2V, employing individual digital pins for each sensor. After powering the sensors, it waits for 15 ms before reading their analog outputs from corresponding analog pins. These analog voltages are converted to digital outputs (ADC values) ranging from 0 to 1023 (for a 10-bit ADC) using the internal analog-to-digital converter. Five readings are averaged to calculate a representative ADC value, which is then converted into measurements for moisture content, NPK levels, pH, and electrical

conductivity using calibration equations developed specifically for this study.

2.4. Control Algorithm Development

The algorithm flowchart of the developed system is shown in Figure 24.

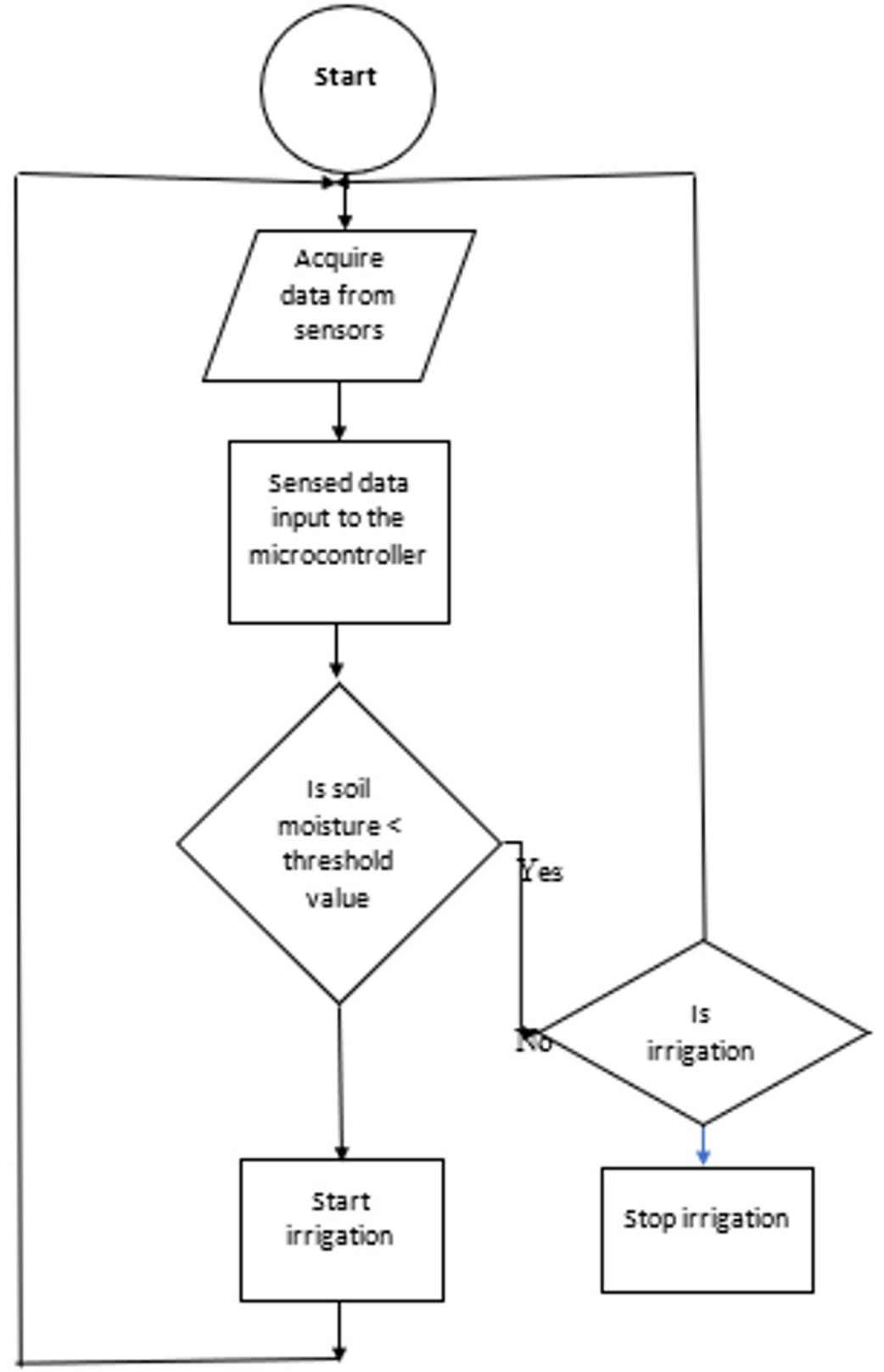

Figure 24. The algorithm flowchart of the system

2.5. User Interface and Data Visualization

The soil data read by the sensors would be displayed through the LCD Display Serial Graphic Display 128x64 ST7920

and be stored in the system data storage for further data analysis and processing on a computer system. Figure 25 shows the real-time parameters of the soil.

Figure 25. Real-time parameters of the soil

2.6. Testing and Evaluation Strategies

To test and evaluate the newly developed system, a calibration equation would be developed for all the soil parameters to be measured by the system. To develop the calibration equation, a laboratory calibration experiment would be conducted, and calibration equations would be derived by correlating the outputs of the sensors measured using the microcontroller against the readings measured in the laboratory or a pro-check meter. Soil samples would be taken at four different depths from different locations on the experimental site for laboratory moisture determination. In addition, soil samples would be taken from each plot for NPK, EC, and pH laboratory determination. In order to evaluate the developed system, statistical evaluation performance criteria in 1 to 3.

$$RMSE = \sqrt{\frac{1}{n}\sum \left(m_i - s_i\right)^2} \quad (1)$$

$$NRMSE = \frac{\sqrt{\frac{1}{n}\Sigma\left(m_i - S_i\right)^2}}{\bar{M}} \quad (2)$$

$$MAE = \frac{1}{n}\sum_{i=1}^{n}\left|m_i - s_i\right| \quad (3)$$

The importance of various metrics such as the coefficient of determination (R^2), root mean square error (RMSE), mean absolute error (MAE), and normalized root mean square error (NRMSE) is significant in data analysis. The m_i and s_i

represent the measured and predicted data, respectively. M represents the average value of m_i, while n is the total number of observations. The coefficient of determination serves as an indicator of model accuracy and is commonly used to compare observed data with model output. A high R^2 value indicates strong model performance, with a value below 0.5 suggesting poor performance. Conversely, an R^2 value above 0.5 signifies a well-performing model. The closer R^2 is to 1, the more precise the model is considered. RMSE, MAE, and NRMSE are employed to evaluate the precision of model predictions in comparison to observed data. Lower MAE and RMSE values indicate more accurate predictions, while an NRMSE value closer to 1 also suggests accuracy in predictions.

2.7. Soil sample laboratory analysis

The experiment utilized the standard laboratory analysis techniques detailed in Table 1 for specific soil chemical and physical properties, including soil pH, total nitrogen (N), available phosphorus, available potassium, and cation exchange capacity (CEC), soil temperature, and moisture content.

Table 1. Summary of laboratory analysis method for soil chemical and physical properties.

Soil properties	Methods
Available P	Olsen 1945 method
Moisture content	Gravimetric method (Oven-dry method)
CEC.	Ammonium acetate method
Soil temperature	Mercury-in-glass thermometer
Total Nitrogen	Kjeldahl digestion method (Bremner, 1996)
pH (1:10)	Digital pH electrometer (Agbede and Ojeniyi, 2009)
Available K	Flame atomic absorption spectrometry (Vogelmann et al., 2010)

3. Results

Comparison between the soil monitoring device measurements and the standard methods. Selected soil properties, which include soil moisture, temperature, nitrogen, phosphorus, potassium, pH, and electrical conductivity, were measured at various points on the experimental site using the newly developed system. Soil samples also were taken and analyzed in the laboratory, and the data obtained were compared with the newly developed system's measurements. Tables 2 to 15 present the error metrics and soil characteristics that were measured at various locations and depths on the experimental site.

Table 2. Soil moisture content measurement

Moisture content determination								
Depth (cm)	Soil sample	Mass of empty can (g)	Mass of empty can + wet soil (g)	Mass of empty can + dry soil (g)	Wet soil (g)	Dry soil (g)	Moisture content (% wb) oven	Moisture content (% wb) measured
10	A1	32.99	162.92	148.41	129.93	115.42	11.17	11.55
10	A2	30.94	156.97	143.2	126.03	112.26	10.93	11.043
10	A3	31.21	136.07	121.46	104.86	90.25	13.93	14.65
10	A4	31.40	111.79	101.46	80.39	70.06	12.85	13.87
20	A12	32.93	132.44	121.42	99.51	88.49	11.07	12.08
20	A13	30.99	112.94	104.76	81.95	73.77	9.98	11.88
20	A14	45.99	211.84	178.82	165.85	132.83	19.91	21.9

Table 3. Soil moisture content measurement error metrics

Moisture content					
R^2	RMSE	MBE	MSE	MAE	NRMSE
0.97	0.14	-0.05	0.02	-0.05	0.28

Table 4. Soil temperature measurements

Soil temperature determination	
Mercury-in-glass thermometer (^oC)	Measured value DS18B20 (^oC)
31.5	31.37
31.5	31.44
31.5	31.44
31.5	31.44
31.5	31.44
31.5	31.5
31.6	31.5
31.6	31.5
32.0	31.94
32.0	31.94
32.0	31.94
32.0	31.94

Table 5. Soil temperature measurement error metrics

Soil temperature					
R2	RMSE	MBE	MSE	MAE	NRMSE
0.98	0.04	0.01	0.00	0.01	0.07

Table 6. Soil pH measurements

Soil pH	
Standard	**Measured**
69.02	71.84
57.35	65.00
38.69	43.20
65.45	68.12

Table 7. Soil pH measurement error metrics

Soil phosphorus					
R2	**RMSE**	**MBE**	**MSE**	**MAE**	**NRMSE**
0.97	1.41	-0.71	1.99	-0.71	0.05

Table 8. Soil nitrogen measurements

Soil nitrogen	
Standard (mg/kg)	**Measured(mg/kg)**
390.65	399.25
291.43	329.56
312.75	319.34
305.32	312.21

Table 9. Soil nitrogen measurement error metrics

Soil nitrogen (mg/kg)					
R^2	**RMSE**	**MBE**	**MSE**	**MAE**	**NRMSE**
0.88	4.30	-2.15	18.49	-2.15	0.05

Table 10. Soil phosphorus measurements

Phosphorus (mg/kg)	
Standard	**Measured**
69.02	79.84
57.35	69.77
38.69	43.20
65.45	68.12

Table 11. Soil phosphorus measurement error metrics

Soil phosphorus					
R^2	**RMSE**	**MBE**	**MSE**	**MAE**	**NRMSE**
0.91	5.41	-2.71	29.27	-2.71	0.15

Table 12. Soil potassium measurements

Potassium (mg/kg)	
Standard	**Measured**
38.50	41.20
19.60	27.30
29.33	31.43
48.61	52.75

Table 13. Soil potassium measurements

Soil Potassium					
R^2	**RMSE**	**MBE**	**MSE**	**MAE**	**NRMSE**
0.96	1.35	-0.68	1.8225	-0.675	0.05

Table 14. Soil electrical conductivity measurements

Electrical conductivity	
standard (us/cm)	**measured (us/cm)**
241.20	254.76
219.56	222.56
305.18	322.00
189.30	215.00

Table 15. Soil electrical conductivity measurement error metrics

Electrical conductivity					
R^2	RMSE	MBE	MSE	MAE	NRMSE
0.96	6.78	-3.39	45.97	-3.39	0.06

5. Discussion

The graphs (a-h) present a comprehensive analysis of the results obtained from evaluating the newly developed integrated soil monitoring system. The system's performance was rigorously assessed by comparing the sensor measurements with standard methods for various soil parameters, including moisture content, temperature, pH, nitrogen, phosphorus, potassium, and electrical conductivity.

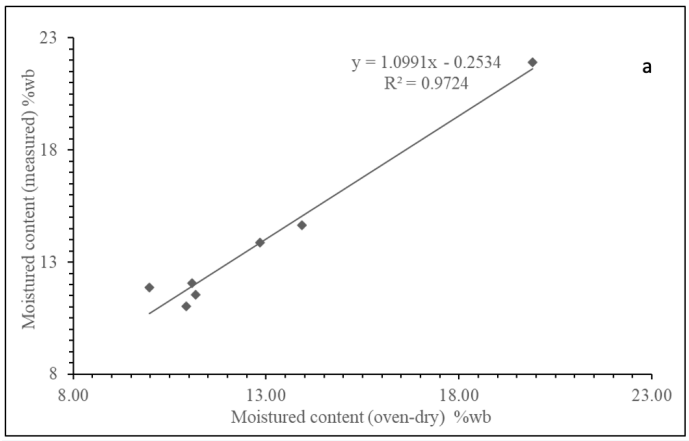

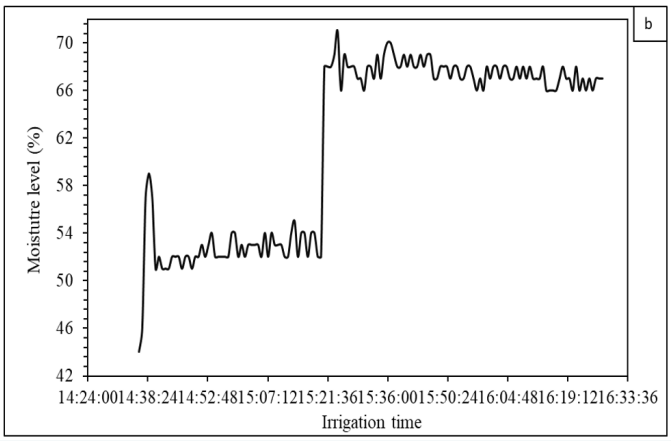

Figures 26-a and 26-b.

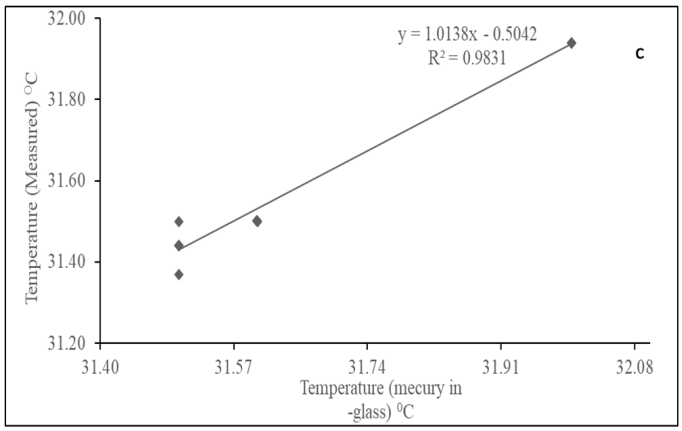

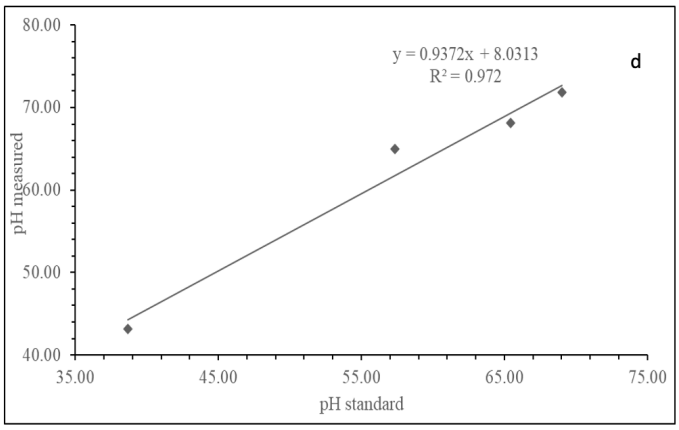

Figures 26-c and 26-d.

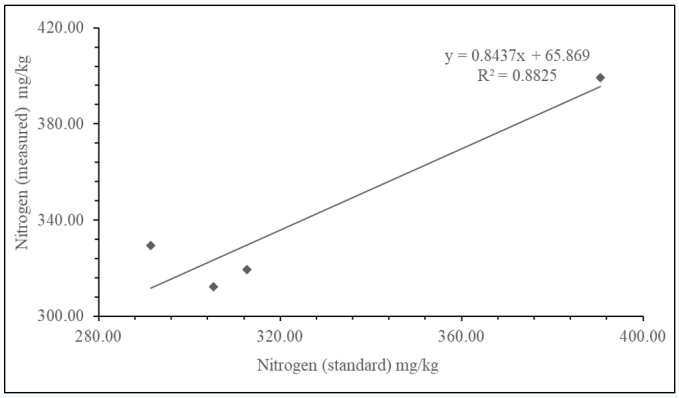

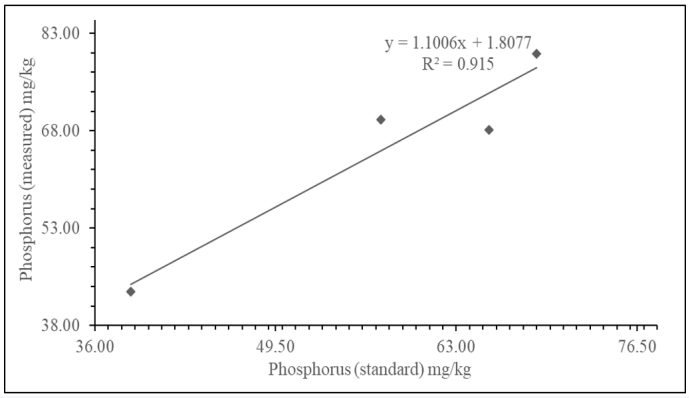

Figures 26-e and 26-f.

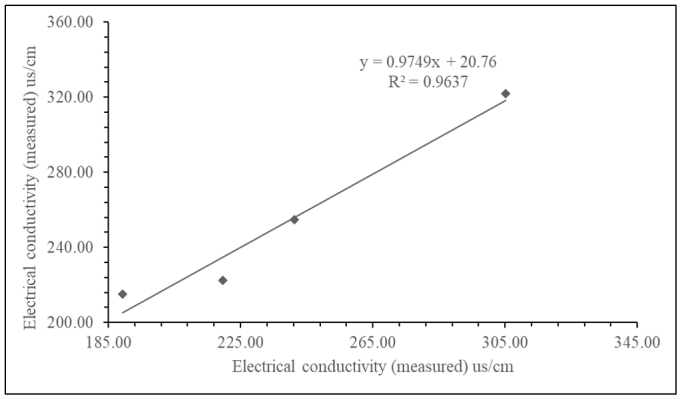

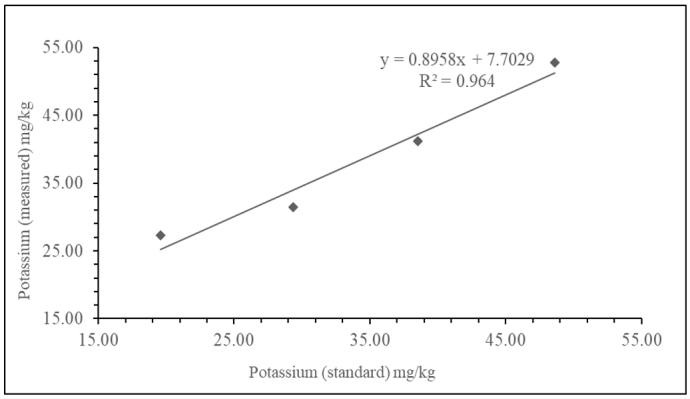

Figures 26-g and 26-h.

Figure 26 (a-h): The results of the soil moisture content measurements obtained from the developed system were compared with the conventional oven-drying method, as shown in Tables 3.1 and 3.2. Table 3.1 and 3.2 showed a good correlation (R^2 = 0.9724) between the measured and actual values, with a low root mean square error (RMSE) of 0.14 and a normalized RMSE of 0.28. The R^2 of 0.9724 in this study is at the higher end of the range reported by Rodrigo et al., suggesting the developed device has slightly better accuracy. Kizito et al. (2008) also reported R^2 values between 0.88-0.97 when calibrating low-cost soil moisture sensors against standard methods. The regression equation developed in this study to convert the measurements taken by the developed system to the standard method is like the calibration approaches used in other studies (Bauer-Marschallinger *et al.*, 2018; Seyfried & Murdock, 2001). All the studies show the feasibility of using low-cost sensors to accurately measure soil moisture compared to standard laboratory methods. The graph presented in (b) shows the soil moisture content over time during an irrigation cycle. The irrigation system maintained the soil moisture content within a target range, as the moisture level stayed relatively close to the preset 70% value, which is the preset threshold. Overall, this graph demonstrates how the soil moisture content changes in response to the irrigation system, reaching and maintaining the target 70% moisture level as intended.

The graph in (c) indicates that soil temperature measurements exhibited an excellent correlation (R^2 = 0.98) between the integrated system and the standard mercury-in-glass thermometer. The RMSE and MBE were minimal, at 0.04°C and 0.01°C, respectively, indicating high accuracy and negligible bias in the temperature measurements. These results are

consistent with the findings of similar studies (Ge *et al.,* 2011; Rosenstock *et al.*, 2013) and validate the system's ability to reliably monitor soil temperature.

The soil pH measurements show a strong correlation (R^2 = 0.97) with the standard values, as shown in graph (d). The high R2 of 0.97 means that approximately 97% of the variability in the pH values obtained from the developed device can be explained by the variability in the standard method. Table 6 suggests a reasonably good fit of the linear model. The statistical metrics in Table 7 suggest that the model has a reasonably good fit to the observed soil pH data. The R^2 value of 0.97 obtained is within the range reported in the literature; Adamchuk et al. (1999) reported R^2 values of 0.98 when calibrating soil pH sensors, while Heiniger et al. (2003) achieved R^2 values around 0.80 for their soil pH sensor calibration. All the studies show the feasibility of using low-cost sensors to accurately measure soil pH compared to standard laboratory methods.

Soil nutrient measurements (Nitrogen, Phosphorus, Potassium): The soil nutrient measurements exhibited strong correlations with the standard values as presented in graphs (e-g). For nitrogen, the R^2 was 0.88; for potassium, the R^2 was 0.91; for phosphorus, R^2 was 0.96. The values from the sensors are within the range reported in similar studies; Adamchuk et al. (2005) reported R^2 values of 0.84 when calibrating an on-the-go soil phosphorus sensor, Viscarra Rossel et al. (2006) achieved R^2 values around 0.89 for predicting soil phosphorus using visible-near infrared spectroscopy, Vaughan et al. (2016) reported R^2 values of 0.90 when calibrating low-cost sensors for soil nitrate, phosphorus, and potassium, and Shaddad *et al.* (2016) obtained R^2 values of 0.75 when using mid-infrared spectroscopy to estimate soil phosphorus. This study and other studies show the feasibility of using low-cost sensors to accurately measure NPK when compared to standard laboratory methods.

The soil electrical conductivity measurements, as shown in graph (h), exhibit a strong linear relationship, as indicated by the high coefficient of determination (R^2 = 0.9637). This suggests that the developed device can accurately measure electrical conductivity in a linear manner compared to the standard method. The slope (0.9749) represents the sensitivity of the developed device, indicating that for every unit increase in the standard electrical conductivity measurement, the developed device measures a 0.9749-unit increase. The high R^2 value (0.9637) suggests that the developed device has the potential to provide accurate electrical conductivity measurements, as it can explain approximately 96.37% of the variance in the standard method measurements.

6. Conclusions

An integrated soil monitoring system that incorporates several soil parameters has been developed. It incorporates the capacity for wireless communication of data collected. The measurements are also used to automatically control irrigation of the soil.

The integration of the sensors with a computer-based user platform allows for comprehensive data collection, analysis, visualization, and interpretation. This enables farmers, agronomists, and other stakeholders to make more informed decisions regarding irrigation, fertilization, and other soil management practices.

The rigorous evaluation of the prototype equipment has validated the accuracy, reliability, and user-friendliness of the system. The wireless transmission capabilities ensure seamless data transfer, while the data analysis and situation monitoring features provide valuable insights to users.

References

- Adamchuk, V.I., Ingram, T.J., Jones, J.W., and Hann, M.J. (1999). Estimating soil conductivity for a spatial measurement of soil properties. ASAE Paper No. 993110, St. Joseph, MI.
- Adamchuk, V.I., Lund, E.D., Sethuramasamyrthy, B., Morgan, M.T., Dobermann, A., and Marx, D.B. (2005). Direct measurement of soil chemical properties on-the-go using ion-selective electrodes. Computers and Electronics in Agriculture, 48(3), 272-294.
- Dai, J., Tang, W., Zheng, Y., Xu, W., Deng, X., Cheng, C., & Wang, Z. (2020). An integrated mobile navigation system for real-time soil NPK data acquisition and soil mapping. Computers and Electronics in Agriculture, 172, 105335.
- Ge, Y., Thomasson, J.A., and Sui, R. (2011). Remote sensing of soil properties in precision agriculture: A review. Frontiers of Earth Science, 5(3), 229-238.
- Heiniger, R.W., McBride, R.G., and Clay, D.E. (2003). Using soil electrical conductivity to improve nutrient management. Agronomy Journal, 95(3), 508-519.
- Miliovsky, M., Lackas, P., & Krkoska, M. (2022). Soil nutrient sensor for nitrogen, phosphorus and potassium content measurement using sensors, 22(8), 2907.
- Muñoz-Huerta, R. F., Guevara-Gonzalez, R. G., Contreras-Medina, L. M., Torres-Pacheco, I., Prado-Olivarez, J., & Ocampo-Velazquez, R. V. (2013). A review of methods for sensing the nitrogen status in plants: advantages, disadvantages and recent advances. Sensors, 13(8), 10823-10843.
- Oborkhale, L., Abioye, A. E., Egonwa, B., & Olalekan, T. (2015). Design and implementation of automatic irrigation control system. *IOSR Journal of Computer Engineering (IOSR-JCE)*, *17*(4), 99–111.
- Padilla, F. M., Gallardo, M., Peña-Fleitas, M. T., Thompson, R. B., & Fernández, M. D. (2018). Proximal optical sensors for nitrogen monitoring in vegetable crops: A review. Sensors, 18(7), 2083.
- Rosenstock, T.S., Chirinda, N., Ollenburger, M., Plant, R.A., and Breuillin, J. (2013). Greenhouse gas emissions from agricultural soil management. In Climate Change and Agriculture: Issues of Agriculture, Resource Management and Risk (pp. 137-157). Nova Science Publishers, Inc.
- Shaddad, S.M., Anchukaitis, K.J., Castañeda, E., Cort, G., Nacci, N., and Harik, G. (2016). Soil spectroscopy: A new approach to assess and monitor soil properties in arid and semi-arid regions. International Journal of Agriculture Innovations and Research, 4(6), 980-986.
- Shibusawa, S. (2001). Soil mapping using the real-time soil spectrophotometer. In*Precision Agriculture'01, Proceedings (on CD-ROM) of the 3rd European Conference on Precision Agriculture*. page *26*, 113–114.
- Tsang, S. W., & Jim, C. Y. (2016). Applying artificial intelligence modeling to optimize green roof irrigation.*Energy and Buildings*, page *127*, 360–369.
- United Nations (2017). World Population to Hit 9.8 billion by 2050, Despite Nearly Universal Lower Fertility Rates. June

2017. Link: https://news.un.org/en/story/2017/06/560022-world-population-hit-98-billion-2050-despite-nearly-universal-lower-fertility

- Vaughan, J.D., Strand, E.J., Kikkert, J.R., and Peterson, G.A. (2016). Soil fertility and soil management. In Western Fertilizer Handbook (pp. 3-19). California Plant Health Association.
- Viscarra Rossel, R.A., Adamchuk, V.I., Sudduth, K.A., McKenzie, N.J., and Lobsey, C. (2006). Proximal soil sensor techniques for measuring soil properties in space and time. In Proceedings of the 18th World Congress of Soil Science, Philadelphia, PA, USA (pp. 9-13).
- Xu, G., Zheng, J., Du, C., & Yuan, P. (2022). Development of a portable soil nutrient sensor based on near-infrared spectroscopy for in-situ measurement of soil nitrogen, phosphorus, and potassium. Sensors, 22(2), 591.